A NUMERICAL CASE STUDY OF ARCTIC STRATUS IN JULY 1975

Sachio OHTA

Department of Sanitary Engineering, Faculty of Engineering, Hokkaido University, Kita-13, Nishi-8, Kita-ku, Sapporo 060

Abstract: A numerical simulation was made of the formation of summertime Arctic stratus clouds in July 1975. As stratus is considered to be generated due to cooling of warm moist air advected over polar ice from the area surrounding the Arctic Ocean, monthly averaged radiosonde data measured at Barrow in July 1975 were used as an initial condition. A model is constructed in which a system of equations for a steady-state planetary boundary layer on cloudy days is transformed into a one-dimensional, time-dependent system of equations by introducing the downstream derivative where the time corresponds to travel time moving with a geostrophic wind velocity. We adopt the smoothed eddy diffusion coefficients based on the experimental formula obtained by KONDO under strong stable conditions in the atmospheric surface layer. Upon using the method of the P_3-approximation for calculating the radiative transfer, radiative effects are incorporated into the model including scattering, absorption and emission of radiation by cloud droplets as well as absorption and emission of radiation by gaseous constituents. Clouds are assumed to be composed of pure liquid water droplets with a measured size distribution. The results of calculation are as follows.

The cloud appears at a height of about 50 m due to lowering of the sea surface temperature. After cloud formation, on account of intense radiative cooling near the top of the cloud, air temperature decreases greatly and a sharp temperature inversion layer is formed in the upper region of the cloud. As the sudden decrease of air temperature enhances condensation of water vapor greatly, the cloud continues developing and gradually rises together with the intense inversion layer.

The simulated liquid water content is two times larger than the measured content and the cloud is not separated into two layers, contrary to observation. The disagreement with the measurement seems to be due to insufficient solar radiative heating in our model cloud which is assumed to be composed of pure liquid water droplets. Therefore, it is important to examine exactly the components of cloud droplets and aerosols which contribute to absorption of solar radiation.

1. Introduction

In summer the Arctic area is frequently covered with stratiform clouds which are called Arctic summer stratus (VOWINCKEI and ORVIG, 1970). JAYAWEERA and OHTAKE (1973) observed these stratus and found after a few days of cloud formation there was seen a sharp temperature inversion in the top half of

the clouds and then an interstice occurred which led to form two cloud layers. The liquid water content was 0.1–0.2 g/m^3 and the cloud droplets had a modal radius of 6–7 μm. These cloud layers have a great influence on the structure of the atmospheric boundary layer and heat balance in the Arctic area.

In our previous paper (OHTA, 1981), a numerical simulation was done on the evolution of Arctic summer stratus, regarding it as an advection fog. The formation of cloud was simulated by incorporating the radiative effects due to cloud droplets according to a P_3-approximation method derived by OHTA and TANAKA (1982) into a steady-state planetary boundary layer model. For an initial condition we used the U.S. standard atmosphere, Arctic, July. The simulated results showed a sharp temperature inversion layer near the top of the cloud, and the inversion layer was lifted with the ascent of the top of cloud. But it was also pointed out that the simulated liquid water content was three times larger than that observed and that the cloud did not separate into two cloud layers contrary to observation. This discrepancy seemed to be attributed partly to the initial condition.

In the present work, therefore, we again simulate the formation of Arctic summer stratus using monthly averaged radiosonde data in July 1975 at Barrow, Alaska as the initial condition. Moreover, as eddy diffusion coefficient for heat, water vapor and liquid water estimated in the previous paper had oversensitiveness against slight change of stability, we use smoothed values of it by taking a moving average.

2. Mathematical Model

As the mathematical model used in this simulation is the same as that in the previous study, only an outline of it is described here. We adopt Cartesian coordinates (x, y, z), where x and y are the horizontal axes and z is the vertical axis. The top of the atmospheric boundary layer z_E, the height of the constant flux layer z_C, and the roughness of the sea surface z_0 are, respectively, supposed to be 2000 m, 20 m and 1 mm. If we assume that air mass, heat, water vapor and liquid water are transported horizontally by wind U, equations for the steady-state planetary boundary layer on cloudy days are given as follows:

$$U\frac{\partial U}{\partial x} = f(V - V_0) - \frac{\partial}{\partial z}(\overline{u'w'}), \tag{1}$$

$$U\frac{\partial V}{\partial x} = -f(U - U_0) - \frac{\partial}{\partial z}(\overline{v'w'}), \tag{2}$$

$$U\frac{\partial \theta_S}{\partial x} = -\frac{\partial}{\partial z}(\overline{\theta_S'w'}) + \left(\frac{P_0}{P}\right)^{0.2857}\left(\frac{\partial T}{\partial t}\right)_R, \tag{3}$$

$$U\frac{\partial q}{\partial x} = -\frac{\partial}{\partial z}(\overline{q'w'}) - \frac{C}{\rho}, \tag{4}$$

$$U\frac{\partial w_d}{\partial x} = -\frac{\partial}{\partial z}(\overline{w_d'w'}) + \frac{\partial}{\partial z}(v_g w_d) + C, \tag{5}$$

where U and V are x- and y-components of wind velocity, U_0 and V_0 are x- and y-components of the geostrophic wind velocity, q the mixing ratio of water vapor,

w_d the liquid water content, $(\partial T/\partial t)_R$ the radiative temperature change, P the pressure, P_0 the surface pressure, C the rate of condensation, ρ the air density and v_g the terminal velocity of cloud droplets. The quantity θ_S is defined by moist static energy h as follows:

$$h=C_p\left(\theta+\frac{L}{C_p}q\right)\equiv C_p\theta s\,,\quad \left(\theta_S\equiv\theta+\frac{L}{C_p}q\right)\,, \tag{6}$$

where C_p is the specific heat of air at constant pressure and L is the latent heat of vaporization. The terms $\overline{u'w'}$ and $\overline{v'w'}$ represent the vertical turbulent transport of x- and y-momentum, and $C_p\,\overline{\theta_S'w'}$, $\overline{q'w'}$ and $\overline{w_d'w'}$ represent the vertical turbulent fluxes of moist static energy, water vapor and liquid water, respectively.

In the atmosphere higher than a few hundred meters the wind U is nearly equal to the geostrophic wind U_0, and we pay attention to the behavior of a stratus cloud which exists at a height of more than 100 m, so that we can linearize the advected terms in eqs.(1)–(5) with a constant geostrophic wind U_0. As in the previous study (OHTA, 1981), we transform these linearized advected terms by using the downward derivative $\delta/\delta t$ as follows:

$$U_0\frac{\partial}{\partial x}[\quad]=\frac{\delta}{\delta t}[\quad]\,. \tag{7}$$

This means that a two-dimensional, steady-state system of eqs.(1)–(5) is transformed to a one-dimensional, time-dependent system of equations. The vertical turbulent transport terms are replaced by the gradient of each quantity by the use of flux-profile relationships. The eddy diffusion coefficients for momentum K_M, and for heat, water vapor and liquid water K_H are given by the experimental formula obtained by KONDO *et al.* (1978). As the values of them are very sensitive to slight change of stability, we smooth them by taking the moving average. Namely, at first we obtain values at each mesh point, $K_H^{(i)}$ $(i=1, 2, \ldots, N)$, by using the experimental formula of KONDO *et al.* (1978), and then take the average as follows:

$$K_{H,i}=(K_H{}^{(i-1)}+K_H{}^{(i)}+K_H{}^{(i+1)})/3\,,\quad (i=2, 3, \ldots, N-1). \tag{8}$$

Thus $K_{H,i}$ is used as the eddy diffusion coefficient for heat, water vapor and liquid water at the i-th mesh point.

This procedure does not have physical meaning, but is performed only to gain smoothed profiles of eddy diffusion coefficients.

3. Treatment of Radiation Processes

In this model the lower boundary is assumed to be a sea surface whose heat capacity is very large or melting pack ice whose temperature is constant (0°C). Therefore, we need not consider the heat balance at the surface. What we must estimate is the radiative temperature change, $(\partial T/\partial t)_R$, in the atmosphere.

In the clear atmosphere, radiative heating due to absorption of solar radiation by gaseous constituents is so small that we can ignore this absorption effect, but radiative cooling due to divergence of infrared radiation is not so small that we can not neglect it. The latter is computed according to RODGERS and WALSHAW

(1966). In the atmospheric window region (8–12 μm), the effect of the continuum absorption due to water dimer is taken into account by using the mean absorption coefficients obtained by BIGNELL *et al.* (1963) and BURCH (1970).

In a cloudy atmosphere, we must take into account absorption and scattering of solar radiation, and absorption, scattering and emission of thermal radiation due to cloud droplets, in addition to absorption and emission due to gaseous constituents. Though the radiative temperature change can be obtained by solving equations of radiative transfer containing these scattering processes, it is very time-consuming to solve these equations exactly by using precise methods such as the matrix method or discrete ordinates method. Therefore, we adopt the method of P_3-approximation for calculating radiative transfer in a cloudy atmospheres, as derived by OHTA and TANAKA (1982). This method can save computational time to a large extent, while its accuracy is sufficient, as shown in that paper.

For the size distribution function of cloud droplets we adopt the measured one shown in Fig. 1, which was obtained by JAYAWEERA and OHTAKE (1973) in the typical summer stratus in the Arctic area. In Fig. 1, $f(r)$ is a frequency distribution function which is normalized to unity, and $Nf(r)\mathrm{d}r$ denotes a number density of cloud droplets between radii r and $r+\mathrm{d}r$, where N is the total number density. With this size distribution function, the relation between N and liquid water content, $w_d(\mathrm{g/m^3})$, is given as

$$N=5.428\times10^8 w_d \quad (\mathrm{cm^{-3}}). \tag{9}$$

A terminal velocity of cloud droplets averaged over this size distribution is obtained as

$$v_g=0.65 \quad (\mathrm{cm/s}). \tag{10}$$

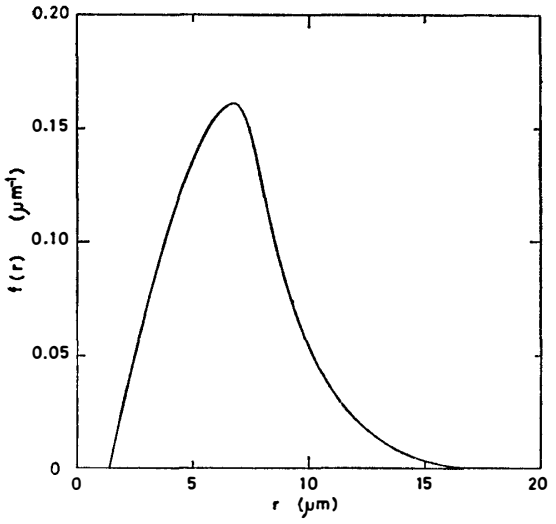

Fig. 1. Frequency distribution function f(r) of cloud droplets in the Arctic summer stratus measured by JAYAWEERA and OHTAKE (1973). r denotes the radius of cloud droplets.

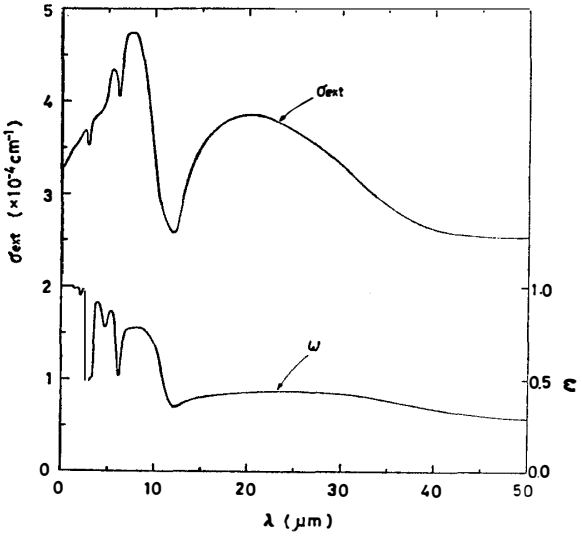

Fig. 2. Extinction cross section σ_{ext} and single scattering albedo ω of the Arctic summer stratus composed of pure liquid water droplets as a function of wavelength λ.

In order to solve equations of radiative transfer, we must know the scattering properties of cloud droplets such as scattering function, volume extinction cross section and albedo for single scattering. These quantities can be calculated from Mie theory by using the size distribution given in Fig. 1 and the complex refractive index of water compiled by HALE and QUERRY (1973). Thus the volume extinction cross section and the single scattering albedo of summertime Arctic stratus which is assumed to be composed of pure liquid water droplets were calculated for $N=$ 100 (cm^{-3}) as shown in Fig. 2.

4. Boundary and Initial Conditions

The solar zenith angle is assumed to remain a constant 74° neglecting the diurnal cycle of solar radiation. The albedo of the sea surface is assumed to be 0.50 according to measurements (HANSON, 1961). As the travel distance x in eqs.(1)–(5) is transformed to the travel time t by the relation

$$x = U_0 t\,, \tag{11}$$

we, hereafter, consider the formation of stratus cloud in (t, z) space. For the numerical integration of the transformed one-dimensional, time-dependent system of equations, we adopt an explicit, forward-time difference with a centered spatial difference scheme.

As we assume that the Arctic summer stratus is generated due to cooling of warm moist air advected over the polar ice from the area surrounding the Arctic Ocean, we adopt profiles of air temperature and relative humidity at Barrow, Alaska as an initial condition. Figure 3 shows monthly averaged profiles of them measured by radiosonde observations at 12:00 at Barrow in July 1975. The surface temperature is 2.5°C and the air temperature reaches the maximum, 6.5°C, at a height of 500 m. The geostrophic wind U_0 is supposed to be 8 m/s according to

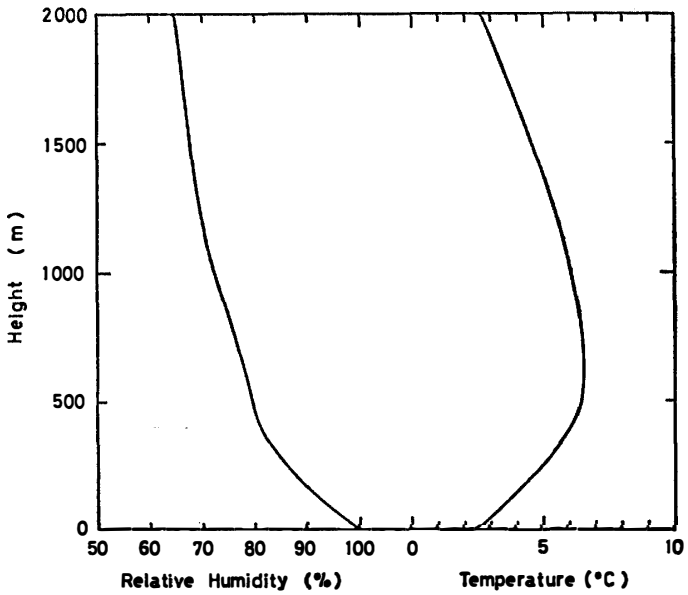

Fig. 3. Initial conditions of air temperature and relative humidity.

the same measurements. The surface temperature is assumed to decrease monotonously from 2.5°C at $t=0$ to 0°C at $t=24$ hours, and after that it remains constant at 0°C. As the surface is considered to be sea water or melting pack ice, surface relative humidity is assumed to be 100%.

5. Results and Discussion

The numerical integration was carried out for a travel time of 48 hours, which corresponds to traveling over a distance of 1382 km with a moving velocity of 8 m/s.

The distribution of liquid water content as a function of height and travel time is shown in Fig. 4. The cloud appears at a height of 50 m. The liquid water content increases with travel time near the top of the cloud and reaches the maximum value of 0.5 g/m^3. The top of the cloud keeps on ascending at a rate of 48 m/hour.

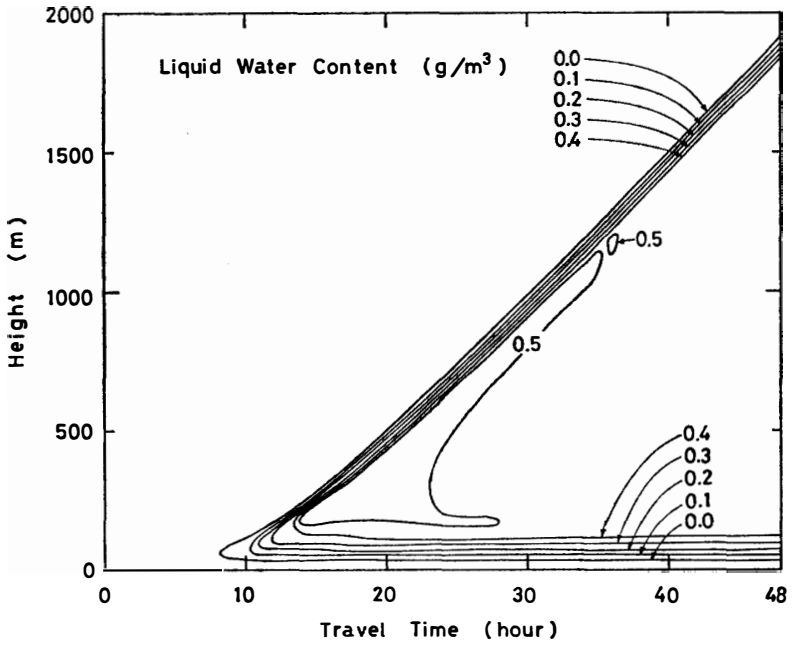

Fig. 4. Distribution of liquid water content as a function of height and travel time.

Vertical distributions of air temperature for each travel time are shown in Fig. 5. The temperature of the sea surface continues to decrease until 24 hours, and after that it remains constant. Meanwhile, in the upper region of the cloud, air temperature continues to decrease rapidly on account of intense radiative cooling near the top of the cloud. On the contrary, the atmosphere above the top of the cloud does not receive an intense radiative cooling effect. Therefore, a sharp temperature inversion layer is formed just below the top of the cloud, and this inversion layer gradually rises with the top of the cloud.

Vertical distributions of the eddy diffusion coefficients for momentum K_M and for heat, water vapor and liquid water K_H are shown in Fig. 6. The values of K_M range from 5×10^3 cm^2/s to 5×10^4 cm^2/s in the whole atmospheric boundary layer.

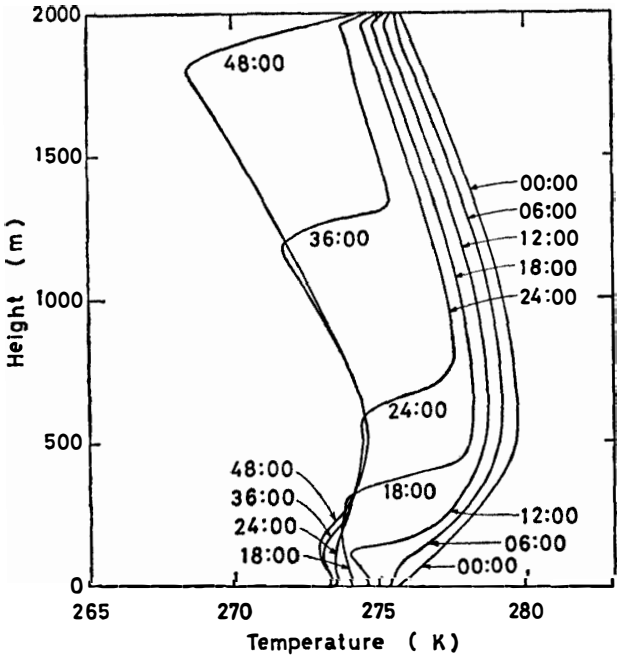

Fig. 5. Vertical distributions of air temperature for each travel time. Numerals in the figure denote the travel time in hours.

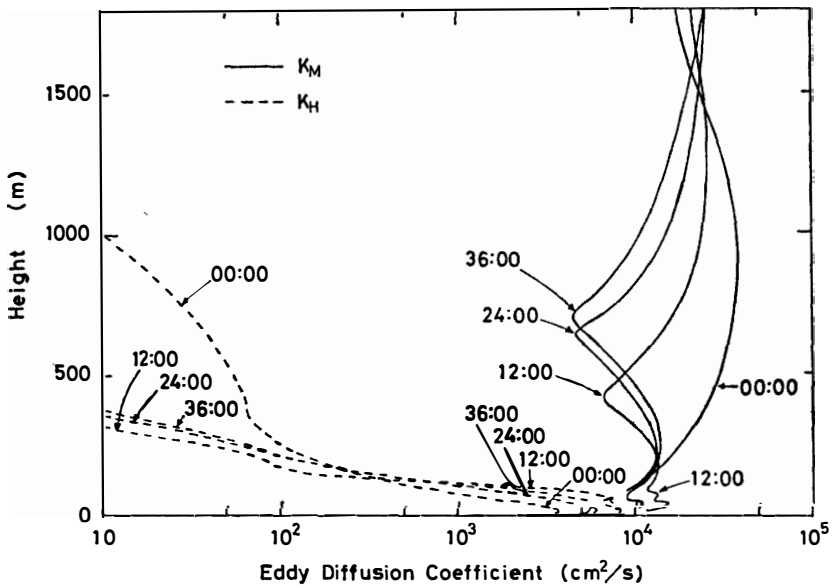

Fig. 6. As in Fig. 5 except for eddy diffusion coefficients for momentum K_M, and for heat, water vapor and liquid water K_H.

These values are reasonable compared with those which have been obtained by measurements in the atmospheric planetary boundary layer. On the other hand, the values of K_H decrease suddenly above the height of a few hundred meters, although they show about the same values as K_M below the height of 100 m where stability is near a neutral condition. From this result it is proved that the eddy diffusion coefficient for momentum does not have a value under $10^3\,cm^2/s$ in the

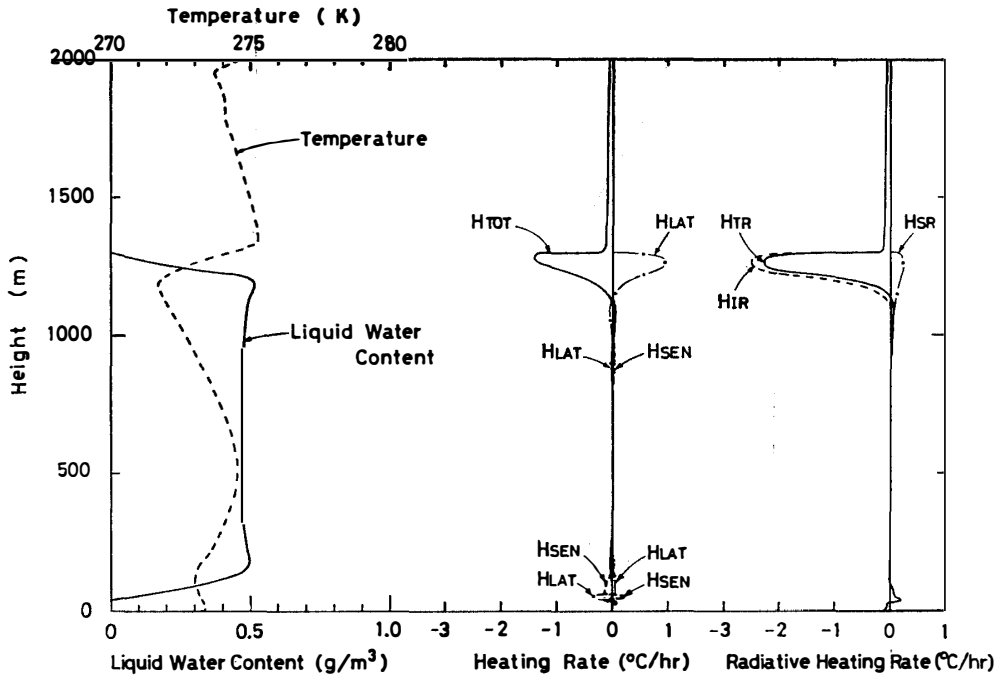

Fig. 7. Vertical distributions of liquid water content, air temperature, total heating rate (H_{TOT}), heating rates due to latent heat (H_{LAT}) and due to sensible heat (H_{SEN}), and total radiative heating rate (H_{TR}), and radiative heating rates due to absorption of solar radiation (H_{SR}) and due to divergence of infrared radiation (H_{IR}).

planetary boundary layer even if the stability is strongly stable, whereas the coefficient for heat, water vapor and liquid water is affected by stability much more than that for momentum.

Figure 7 shows vertical distributions of liquid water content, air temperature, total heating rate (H_{TOT}), heating rates due to latent heat of condensation (H_{LAT}) and due to sensible heat (H_{SEN}), and total radiative heating rate (H_{TR}), radiative heating rates due to absorption of solar radiation (H_{SR}) and due to divergence of infrared radiation (H_{IR}) at the travel time of 36 hours (travel distance $x = 1037$ km). The top of the cloud reaches a height of 1300 m, and the cloud has a maximum density of 0.51 g/m^3 at a height of 1190 m. The minimum air temperature is 271.7 K at a height of 1200 m, from where the temperature shows an intense inversion to the top of the cloud. In this inversion layer, the radiative heating rate due to absorption of solar radiation has a maximum value of 0.25°C/hour, whereas the radiative cooling rate due to divergence of infrared radiation has a maximum value of 2.50°C/hour. Consequently, the total radiative heating rate has a maximum value of −2.25°C/hour at a height of 1260 m. On account of this intense radiative cooling, the air temperature in the inversion layer is forced to go down greatly and water vapor condenses there. The heating rate due to condensation is 0.95°C/hour. As the eddy diffusion coefficient for heat is very small above the height of a few hundred meters, the heating rate due to convergence of the sensible heat flux in this inversion layer is very small compared with the radiative or latent

heating there.

Ultimately, the total heating rate becomes $-1.30°C$/hour in the layer of height 1250 m to 1300 m. This intense cooling just below the top of the cloud causes an extreme drop of air temperature and enhances the condensation of water vapor in the inversion layer. As the radiative cooling rate in the cloud-free layer just above the top of the cloud is about two times that in the layer far away from the top of the cloud and the relative humidity in the cloud-free layer becomes high near the top of the cloud, the air temperature just above the top of the cloud approaches the dew point more rapidly than that of the other layer above the cloud. Thus the water vapor just above the top of the cloud condenses to form new cloud layers and the top of the cloud ascends gradually. Incidentally, in our calculation, at the top of the cloud where there is no liquid water content ($w_d=0$) we adopt a value of radiative temperature change obtained in the layer which is the upper half of the pre-divided layer just below the top of the cloud. Therefore, we may assign a larger radiative cooling rate at the top of the cloud, and the top of it may ascend faster than the observed rate.

At the base of the cloud, water droplets are transported downward due to turbulence and gravitational settling. Evaporation of these droplets causes cooling at the rate of $0.35°C$/hour. However, this cooling is compensated for by radiative heating due to the convergence of infrared radiation and heating due to the convergence of sensible heat flux there.

In our previous study (OHTA, 1981), the simulated liquid water content was three times larger than the measured content and the cloud was not separated into two layers, contrary to observation. Before the simulation this time, the author presumed that if we used the new initial condition in which the relative humidity and mixing ratio of water vapor had larger values at the height from 100 m to 1000 m (shown in Fig. 3) than in the previous case, we could obtain more plausible simulated results. Specifically, as there is more moist air in the planetary boundary layer than in the previous case, condensation occurs more rapidly in the cloud-free layer just above the top of the cloud and the top of the cloud ascends faster. As the cloud has the maximum cooling rate just below its top, if its top ascends faster, the air temperature in the cloud does not fall more than in the previous case and the amount of condensation of water vapor becomes less. Therefore, the author presumed that we might obtain a thinner cloud than in the previous case.

Comparing the results of this simulation with that of previous study, the liquid water content formed in this simulation decreases slightly and the profiles of eddy diffusion coefficients are smoother. However, compared with the measurements by JAYAWEERA and OHTAKE (1973), the liquid water content is still two times larger than that observed and an interstice in the cloud does not seem to occur two days after formation of cloud.

These results show that the discrepancy between our simulated results and measurements are not due to the initial condition. According to the simulation of Arctic summer stratus by HERMAN and GOODY (1976), they concluded that a little liquid water content and the occurrence of an interstice in Arctic summer stratus are caused by the intense heating due to absorption of solar radiation in the cloud.

However, if cloud droplets are composed of only pure liquid water, the single scattering albedo is 0.99999 in the visible region of the spectrum (0.3–0.7 μm) and 0.999 in the region of the spectrum from 0.7 μm to 1.25 μm, as shown in Fig. 2 in our study. The values below 0.999 appear only just in the remaining region of the spectrum (1.25–4.0 μm) in Fig. 2, and most of heating in the cloud due to absorption of solar radiation is caused in this region of the spectrum. But, as only 20% of solar energy is contained there, solar heating in cloud composed of pure liquid water droplets is much smaller than infrared cooling as shown in Fig. 7. Namely, if the cloud is supposed to be composed of pure liquid water droplets, an observed feature of Arctic summer stratus will not be simulated.

On the other hand, HERMAN (1977) observed the radiative properties of Arctic summer stratus in the solar region of the spectrum. According to his measurements, the single scattering albedo in the visible region is 0.994–0.998, and in the near-infrared region 0.990–0.993. This means that the summertime Arctic stratus cloud is not composed of only pure liquid water droplets, but of a mixture of liquid water and absorptive materials such as soot or hematite particles.

If we adopt these observed values of the single scattering albedo, our simulation may be able to yield plausible results. Consequently, in order to make clear the mechanism of formation and persistence of Arctic summer stratus, it is important to examine exactly those components of cloud droplets and aerosols which contribute to absorption of solar radiation in the Arctic area.

Acknowledgments

The author wishes to express his gratitude for guidance and encouragement received from Prof. Masayuki TANAKA, Upper Atmosphere Research Laboratory, Tohoku University and Prof. Toshiichi OKITA, Faculty of Engineering, Hokkaido University.

References

BIGNEL, K., SAIEDY, F. and SHEPPARD, P. A. (1963): On the atmospheric infared continuum. J. Opt. Soc. Am., **53**, 466–479.

BURCH, D. E. (1970): Investigation of the absorption of infrared radiation by atmospheric gases. Semi-annual Tech. Rep. AFCRL Publ. U-4784, Contract No. F19628-69-C-0263.

HALE, G. M. and QUERRY, M. R. (1973): Optical constants of water in the 200-nm to 200-μm wavelength region. Appl. Opt., **12**, 555–563.

HANSON, K. J. (1961): The albedo of sea-ice and ice islands in the Arctic Ocean Basin. Arctic, **14**, 188–196.

HERMAN, G. F. (1977): Solar radiation in summertime Arctic stratus clouds. J. Atmos. Sci., **34**, 1423–1432.

HERMAN, G. and GOODY, R. (1976): Formation and persistence of summertime Arctic stratus clouds. J. Atmos. Sci., **33**, 1537–1553.

JAYAWEERA, K. O. L. F. and OHTAKE, T. (1973): Concentration of ice crystals in arctic stratus clouds. J. Rech. Atmos., **7**, 199–207.

KONDO, J., KANECHIKA, O. and YASUDA, N. (1978): Heat and momentum transfer under strong stability in the atmospheric surface layer. J. Atmos. Sci., **35**, 1012–1021.

OHTA, S. (1981): A numerical study of the formation of summertime Arctic stratus clouds. Mem. Natl Inst. Polar Res., Spec. Issue, **19**, 104–117.

OHTA, S. and TANAKA, M. (1982): A P_3-approximation method as applied to foggy and cloudy atmospheres. To be published in J. Quant. Spectrosc. Radiat. Transfer.

RODGERS, C. D. and WALSHAW, C. D. (1966): The computation of infrared cooling rate in planetary atmospheres. Q. J. R. Meteorol. Soc., **92**, 67–92.

VOWINCKEI, E. and ORVIG, S. (1970): The climates of the North Polar Basin. Climates of Polar Regions, ed. by S. ORVIC. Amsterdam, Elsevier, 129–252 (World Survey of Climatology, Vol. 14).

(Received April 26, 1982; Revised manuscript received July 23, 1982)